

Fast Robust Methods for Singular State-Space Models

Jonathan Jonker^a, Aleksandr Aravkin^b, James Burke^a, Gianluigi Pillonetto^d,
Sarah Webster^c.

^a*Department of Mathematics, University of Washington*

^b*Department of Applied Mathematics, University of Washington*

^c*Applied Physics Lab, University of Washington*

^d*Department of Information Engineering, University of Padova*

Abstract

State-space models are used in a wide range of time series analysis formulations. Kalman filtering and smoothing are workhorse algorithms in these settings. While classic algorithms assume Gaussian errors to simplify estimation, recent advances use a broader range of optimization formulations to allow outlier-robust estimation, as well as constraints to capture prior information.

Here we develop methods on state-space models where either innovations or error covariances may be singular. These models frequently arise in navigation (e.g. for ‘colored noise’ models or deterministic integrals) and are ubiquitous in auto-correlated time series models such as ARMA. We reformulate all state-space models (singular as well as nonsingular) as constrained convex optimization problems, and develop an efficient algorithm for this reformulation. The convergence rate is *locally linear*, with constants that do not depend on the conditioning of the problem.

Numerical comparisons show that the new approach outperforms competing approaches for *nonsingular* models, including state of the art interior point (IP) methods. IP methods converge at superlinear rates; we expect them to dominate. However, the steep rate of the proposed approach (independent of problem conditioning) combined with cheap iterations wins against IP in a run-time comparison. We therefore suggest that the proposed approach be the *default choice* for estimating state space models outside of the Gaussian context, regardless of whether the error covariances are singular or not. To highlight the modeling capabilities of singular models, we include a featured application for smoothing sea survey data.

1 Introduction

The linear state space model is widely used in tracking and navigation [8], control [1], signal processing [2], and other time series [11,21]. The model assumes linear relationships between latent states with noisy observations:

$$\begin{aligned} x_1 &= x_0 + w_1 \\ x_k &= G_k x_{k-1} + w_k \quad k = 2, \dots, N \\ y_k &= H_k x_k + v_k \quad k = 1, \dots, N, \end{aligned} \tag{1}$$

where x_0 is a given initial state estimate, x_1, \dots, x_N are unknown latent states with known linear process models G_k , and y_1, \dots, y_N are observations obtained using

Email addresses: jonkerjo@uw.edu (Jonathan Jonker), saravkin@uw.edu (Aleksandr Aravkin), jvburke@uw.edu (James Burke), giapi@dei.unipd.it (Gianluigi Pillonetto), swebster@apl.washington.edu (Sarah Webster).

known linear models H_k . It does not make sense to observe data that is not in the range of H_k ; so we assume that H_k are surjective.

The errors w_k and v_k are assumed to be mutually independent random variables with known covariances Q_k and R_k . In tracking and navigation, the end goal is the estimation of the latent states $\{x_k\}$. In other settings, such as autocorrelated time series models (e.g. Holt-Winters c.f. [11], ARMA c.f. [21]), estimating the state is a necessary step to evaluate a conditional likelihood that informs additional parameters on which G_k , H_k , Q_k and R_k may depend. In either setting, estimating the state sequence $\{x_k\}$ efficiently is essential.

Singular Covariances. We are particularly interested in models where Q_k and R_k may be singular. These models arise in all settings where state-space formulations

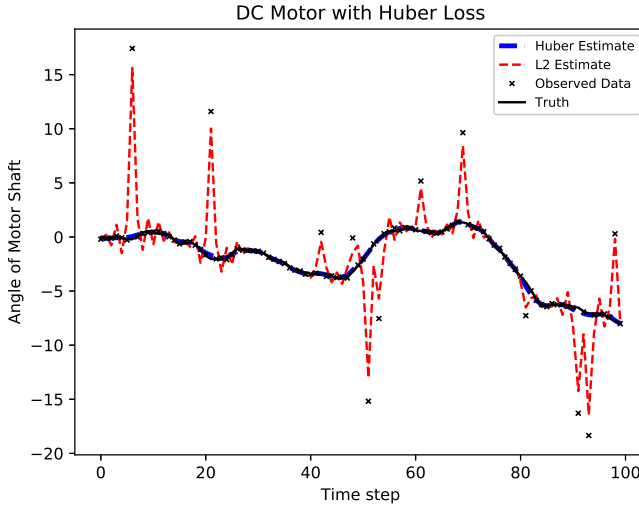


Fig. 1. DC motor (2) with outliers, generated from a Gaussian with high variance. The process covariance Q is singular, but the standard RTS smoother still finds the linear minimum variance estimate (red). Our reformulation allows using robust penalties (in this case, Huber) with a singular covariances to obtain a better solution (blue).

are used¹. In navigation, the simplest example is the DC motor [15, pp. 95-97]:

$$\begin{aligned} x_{k+1} &= \begin{pmatrix} 0.7 & 0 \\ 0.084 & 1 \end{pmatrix} x_k + \begin{pmatrix} 11.81 \\ 0.62 \end{pmatrix} (c_k + d_k) \\ y_k &= \begin{pmatrix} 0 & 1 \end{pmatrix} x_k + v_k. \end{aligned} \quad (2)$$

Here, y_k are noisy samples of the angle of the motor shaft, c_k are known inputs, and d_k denote random process disturbances. The covariance matrix Q_k associated to w_k has dimension 2 and rank 1. This example is general in the sense that singular models appear any time a single source of error is integrated into multiple states; a pervasive phenomenon in navigation models [2].

The classic Kalman filter [13] and RTS smoother [19] assume that w_k, v_k are Gaussian, and find the minimum variance estimates of the state, conditioned on the observations [2]. More generally, the RTS smoother finds the linear minimum variance estimator. This procedure is well defined for singular covariances Q_k and R_k , and the smoother can be derived as a sequence of least squares projections [3]. However, when the noise is not Gaussian (e.g. in the presence of outliers), these estimates are not satisfactory; and far better estimates can be obtained through a maximum a posteriori (MAP) estimator [4]. The results in Figure 1 are obtained using the Huber

¹ State space formulations for AR/MA/ARMA and Holt-Winters models are always singular.

loss, which is a convex penalty function that is quadratic near the origin, but with linear tails:

$$\rho(x) = \begin{cases} \frac{1}{2}x^2 & \text{if } |x| \leq \kappa \\ \kappa(|x| - \frac{1}{2}\kappa) & \text{if } |x| \geq \kappa \end{cases}$$

Implementing a general MAP estimator for singular covariances requires a new approach.

General Kalman Smoothing. Classic Gaussian formulations fail when outliers are present in the data, are unable to track abrupt state changes, and cannot incorporate side information through constraints. To develop effective approaches in these cases, generalized Kalman smoothing formulations have been proposed in the last few years, see [4] and the references within. The conditional mean is no longer tractable to compute these estimates, and *maximum likelihood* (ML) formulations are much more natural. The general form of Kalman smoothing considered in [4] is given by

$$\min_{x \in X} \sum_{i=0}^n \rho_1(Q_k^{-1/2}(x_k - G_k x_{k-1})) + \rho_2(R_k^{-1/2}(y_k - H_k x_k)), \quad (3)$$

where ρ_1, ρ_2 are convex penalties, and $x \in X$ is a set of state-space constraints. The two approaches agree in the nonsingular Gaussian case, where (3) becomes a least squares (LS) problem that can be solved with classic RTS or Mayne-Fraser smoothing algorithms [4].

Contribution. We develop a reformulation that extends (3) to **singular covariance models** Q_k and R_k , and implement a Douglas-Rachford splitting (DRS) algorithm to solve this reformulation. The result shown in Figure 1 uses Huber penalties for process and measurement, with the singular process covariance model from (2).

Efficiency of the estimation algorithm is a key requirement. We analyze the DRS for the singular reformulation, and show that it converges locally linearly for any piecewise linear quadratic (PLQ) loss, and that the rate does not depend on the conditioning of the system. This means that **even when the model is non-singular, the new approach is potentially much faster** than first-order and second-order methods for (3). The advantage increases as the models become more ill-conditioned. We illustrate this point with numerical examples.

The paper proceeds as follows. In Section 2 we discuss prior approaches to singular models. In Section 3, we develop a constrained reformulation of (3), building on early work of [18] for singular least squares. In Section 4, we show how to efficiently optimize a wide range of singular smoothing problems using DRS. The algorithm we use has a *local linear rate of convergence* for any

piecewise linear-quadratic penalties ρ_1, ρ_2 in (3), and each iteration is efficiently and stably computed by exploiting dynamic problem structure. We compare the new algorithm to first-order methods, L-BFGS, and IP-solve, a toolbox specifically developed for PLQ Kalman smoothing (for nonsingular formulations). In Section 5, we present a navigation model that uses singular errors. In Section 6 we apply the methodology to analyze sea-surface survey data.

2 Related Work

Several approaches in the literature deal with singular models. We give a brief description and references for each. To ground the discussion, consider tracking a particle moving along a smooth path in space, where state comprises velocity and position. Singular models arise naturally in this situation. One approach models acceleration α as a stochastic driving term for both states:

$$\begin{aligned} x_{k+1} &= x_k + \Delta t \dot{x}_k + \frac{1}{2} \Delta t^2 \alpha_k \\ \dot{x}_{k+1} &= \dot{x}_k + \Delta t \alpha_k. \end{aligned} \quad (4)$$

Alternatively, we can model velocity as subject to error, and position as a deterministic integral:

$$\begin{aligned} x_{k+1} &= x_k + \Delta t \dot{x}_k \\ \dot{x}_{k+1} &= \dot{x}_k + \epsilon_k. \end{aligned} \quad (5)$$

In both models, the process covariance matrices Q_k have rank one.

Using the original Kalman filter. In the linear Gaussian setting, the original Kalman filter does not require Q and R to be invertible. Applying the Kalman filter (and RTS smoother) will return the minimum variance estimate for singular innovation/measurement errors [2]. The limitation is that we cannot consider the general optimization context (3), which we need to incorporate robustness to outliers and constraints for prior information (see example in Figure 1).

Changing the model. A common approach is to modify the model to make Q_k, R_k nonsingular. Treating (5) as a discretization of a stochastic differential equation (SDE), many authors opt for a nonsingular error model [12,17,9,7]

$$Q_k = \begin{bmatrix} \Delta t_k & \Delta t_k^2/2 \\ \Delta t_k^2/2 & \Delta t_k^3/3 \end{bmatrix},$$

derived by computing the variance of a discretized process noise term, similar to what is done in Section 5, see (28). The approach has limitations for navigation models with high-dimensional states driven by low-dimensional errors. The low-dimensional error structure

should simplify estimation, but instead this approach introduces full-dimensional and ill-conditioned Q_k . In addition, making Q_k nonsingular is antithetical to state-space formulations for models such as ARMA, which use singularity to enforce auto-regressive constraints.

Change of coordinates. When only the R_k are singular, [2] suggests making a change of coordinates in the measurement variables and then projecting to remove the extra dimensions. The projections might vary between time points, and the approach does not extend to the case where the singularity is in the state equation, as in (4) or (5).

Pseudo-inverse with orthogonality constraints. The formulation that is closest to ours is that of [16], who replace the inverse of Q_k by a pseudo-inverse, and add orthogonality constraints (namely that projection onto the null space of Q_k is zero). With potentially singular Q_k and R_k , the maximum likelihood estimate for the Gaussian/LS model can be formulated as

$$\begin{aligned} \min_x \sum_k & \|Q_k^{\dagger/2}(x_k - G_k x_{k-1})\|^2 + \|R_k^{\dagger/2}(y_k - H_k x_k)\|^2 \\ \text{s.t. } & Q_k^{\perp}(x_k - G_k x_{k-1}) = 0, \quad R_k^{\perp}(y_k - H_k x_k) = 0 \\ & \text{for all } k = 1, \dots, N, \end{aligned} \quad (6)$$

see [4, Appendix A]. This requires computing both the pseudo-inverse and orthogonality constraints.

Constrained reformulation. The reformulation we choose was first suggested by Paige [18]. Given the singular least squares problem

$$\min_x \|Q^{\dagger/2}(Ax - b)\|^2 \quad \text{s.t.} \quad Q^{\perp}(Ax - b) = 0,$$

we can instead write it as

$$\min_{x,u} \|u\|^2 \quad \text{s.t.} \quad Q^{1/2}u = Ax - b. \quad (7)$$

It is easy to see (6) and (7) are equivalent; the latter is more elegant, and only requires computing a root of Q , rather than using both Q and Q^{\dagger} . When Q is invertible, both formulations are equivalent to

$$\min_x \|Q^{-1/2}(Ax - b)\|^2.$$

Crucially, separating the affine constraint from the original penalty has computational advantages in the general fitting context. We discuss these advantages in the context of the convergence analysis for the proposed method, and illustrate them using a numerical comparison.

3 General Singular Kalman Smoothing

Following the ideas proposed by [16], we introduce variables u_k for the normalized process innovations, and t_k for the normalized residuals. We also introduce a penalty ρ_3 for the states. In the examples we consider, ρ_3 is an indicator function for the known feasible regions X :

$$\delta_X(x_k) = \begin{cases} 0 & x_k \in X_k \\ \infty & x_k \notin X_k \end{cases}.$$

The reformulated singular Kalman smoothing problem is given by

$$\begin{aligned} \min_{u,t,x} & \sum_{k=1}^N \rho_1(u_k) + \rho_2(t_k) + \rho_3(x_k) \\ \text{s.t.} & Q_k^{1/2} u_k = G_k x_{k-1} - x_k \\ & R_k^{1/2} t_k = y_k - H_k x_k \end{aligned} \quad (8)$$

This problem is equivalent to (3) when Q_k and R_k are nonsingular. For singular models, (8) requires only that roots $Q^{1/2}$ and $R^{1/2}$ are available.

Constrained Robust DC motor. Recall the DC motor example in the introduction (2). The data used to make Figure 1 is contaminated with outliers, so we want to use the robust Huber loss for the measurement errors. Suppose we also know upper and lower bounds on the states, $B := \{x : l \leq x \leq u\}$. Then the formulation of the robust constrained singular DC motor is given by

$$\begin{aligned} \min_{u,t,x} & \sum_{k=1}^N \|u_k\|^2 + \rho_h(t_k) + \delta_B(x_k), \\ & \begin{bmatrix} 11.8 & 0 \\ 0.62 & 0 \end{bmatrix} u_k = x_{k+1} - \begin{pmatrix} 0.7 & 0 \\ 0.084 & 1 \end{pmatrix} x_k - \begin{pmatrix} 11.81 \\ 0.62 \end{pmatrix} c_k \\ & \sigma t_k = (a_k - x_{2,k}). \end{aligned}$$

Structure-preserving Reformulation. We now rewrite (8) into a more compact and structure-revealing form. Define

$$\begin{aligned} D_i &= \begin{pmatrix} Q_i^{1/2} & 0 & I \\ 0 & R_i^{1/2} & H_i \end{pmatrix} \text{ for } i = 1, \dots, N, \\ B_j &= \begin{pmatrix} 0 & 0 & -G_{j+1} \\ 0 & 0 & 0 \end{pmatrix}, \text{ for } j = 1, \dots, N-1, \end{aligned} \quad (9)$$

and let

$$A = \begin{pmatrix} D_1 & 0 & \dots & 0 \\ B_1 & D_2 & 0 & \vdots \\ 0 & \ddots & \ddots & 0 \\ 0 & 0 & B_{N-1} & D_N \end{pmatrix}. \quad (10)$$

Define also

$$\begin{aligned} z^T &= (u_1^T \ t_1^T \ x_1^T \ \dots \ u_N^T \ t_N^T \ x_N^T) \\ \hat{w}^T &= (x_0^T \ y_1^T \ 0 \ y_2^T \ \dots \ 0 \ y_N^T). \end{aligned} \quad (11)$$

Now we can write (8) compactly as

$$\begin{aligned} \min_z & \rho(z) \text{ s.t. } Az = \hat{w}, \\ \rho(z) &= \sum_{k=1}^N \rho_1(u_k) + \rho_2(t_k) + \rho_3(x_k). \end{aligned} \quad (12)$$

The order of blocks in z is chosen to the constraint matrix A in (10) lower block bi-diagonal.

The constraint $Az = \hat{w}$ raises a natural question: when is a singular Kalman smoothing model solvable? Clearly we want $\hat{w} \in \text{Ran}(A)$, but we want this condition to hold for any realization of the data \hat{w} , so we want to know when A is surjective. We can characterize this condition precisely in terms of a simple conditions on the individual blocks R_i, Q_i, H_i .

Theorem 3.1 (Surjectivity of A) *The following are equivalent.*

- (1) A is surjective.
- (2) Each block D_i is surjective.
- (3) $\text{null} \left(\begin{bmatrix} Q_i^{1/2} & 0 \\ 0 & R_i^{1/2} \end{bmatrix} \right) \subset \text{Ran} \left(\begin{bmatrix} I \\ H_i \end{bmatrix} \right)$ for all i .
- (4) $R_i + H_i (I - (Q_i + I)^{-1}) H_i^T$ is invertible for all i .

Proof: Conditions 2, 3, 4 are easily seen to be equivalent. To see that 2 and 3 are equivalent, note that the matrix

$$\begin{bmatrix} Q_i^{1/2} & 0 \\ 0 & R_i^{1/2} \end{bmatrix}$$

is symmetric, so its nullspace is perpendicular to its range. Therefore surjectivity of D_i is equivalent to the condition that the range of $\begin{bmatrix} I \\ H_i \end{bmatrix}$ covers this nullspace.

To see the equivalence of 2 and 4, recall that B is surjective if and only if BB^T is invertible, so D_i is surjective

exactly when the matrix

$$\begin{bmatrix} Q_i + I & H_i^T \\ H_i & R_i + H_i H_i^T \end{bmatrix}$$

is invertible. $Q_i + I$ is always invertible, so invertibility of the block 2×2 matrix is equivalent to the invertibility of the Schur complement $R_i + H_i (I - (Q_i + I)^{-1}) H_i^T$.

It remains to show that conditions 1 and 2 are equivalent. We proceed by induction on N . The base case is trivial, since for $N = 1$, $A = D_1$. For the inductive case, consider that for $N = k$ the result holds, and write the $N = k + 1$ case as

$$\begin{bmatrix} A_k & 0 \\ [0 & B_k] D_{k+1} \end{bmatrix} \begin{bmatrix} z_1 \\ z_2 \end{bmatrix} = \begin{bmatrix} w_1 \\ w_2 \end{bmatrix},$$

and assume that A_k is surjective. We then know that there exists z_1 that satisfies $A_k z_1 = w_1$. The second row can now be written explicitly as

$$D_{k+1} z_2 = w_2 + G_{k+1} x_k,$$

where x_k is the last component of z_1 . Thus A_{k+1} is surjective exactly when D_{k+1} is, as desired.

4 Douglas-Rachford Splitting for General Singular Kalman Smoothing

Consider problem (12) as a sum of two functions, $\rho + g$, with ρ as in (12) and g the indicator function of the affine constraint $Az = \hat{w}$:

$$g(z) = \begin{cases} 0 & Az = \hat{w} \\ \infty & Az \neq \hat{w} \end{cases}. \quad (13)$$

Douglas-Rachford splitting (DRS) is a classic algorithm for this problem. For a convex function f , define the proximity operator (see e.g. [10]) as

$$\text{prox}_{\alpha f}(\zeta) = \arg \min_x \frac{1}{2\alpha} \|\zeta - x\|^2 + f(x).$$

The DRS algorithm for (12) detailed in Algorithm 1.

Algorithm 1 Douglas-Rachford Splitting (DRS)

Require: Initialize at any z^0, ζ^0 .

- 1: **loop**
- 2: $z^k = \text{prox}_{\tau g}(z^{k-1} - \tau \zeta^{k-1})$
- 3: $\zeta^k = \text{prox}_{\sigma \rho^*}(\zeta^{k-1} + \sigma(2z^k - z^{k-1}))$

Implementing DRS in our case requires computing two proximity operators at each iteration. One proximity operator is prox_{ρ^*} , where ρ^* denotes the *convex conjugate*:

$$\rho^*(y) = \sup_x \langle y, x \rangle - \rho(x)$$

The prox of a function is related to the prox of its conjugate by Moreau's decomposition:

$$\text{prox}_\rho(x) + \text{prox}_{\rho^*}(x) = x.$$

Thus it suffices to compute prox_ρ . The function ρ captures all user-supplied models, including losses used process and measurement transitions, as well as penalties or constraints on the state, ρ_1, ρ_2 and ρ_3 . The proximity operators of these individual elements must be provided; then prox_ρ is a stack of these input functions. Proximity operators for many common functions are easily available [10], and we include a small library with our implementation².

The second proximity operator is prox_g , which is independent of user choice for process, measurement, and prior models:

$$\text{prox}_g(\eta) = \arg \min_{Az = \hat{w}} \frac{1}{2} \|\eta - z\|^2.$$

This is a simple quadratic with affine constraints, with optimality conditions given by

$$\begin{bmatrix} I & A^T \\ A & 0 \end{bmatrix} \begin{bmatrix} z \\ \nu \end{bmatrix} = \begin{bmatrix} \eta \\ \hat{w} \end{bmatrix}.$$

There are many ways to solve this system. We opt to reduce the problem to solving a block tridiagonal system:

$$\begin{bmatrix} I & A^T \\ 0 & AA^T \end{bmatrix} \begin{bmatrix} z \\ \nu \end{bmatrix} = \begin{bmatrix} \eta \\ A\eta - \hat{w} \end{bmatrix}$$

We solve $AA^T\nu = A\eta - \hat{w}$, then back-substitute to get the optimal z . The system AA^T does not change over iterations; only the right hand side changes. We can therefore compute a single factorization, then use it in each iteration. Since A is block bidiagonal (10), AA^T is block tridiagonal; when A is surjective, AA^T is nonsingular, and we can find a lower block diagonal Cholesky factorization L with $LL^T = AA^T$:

$$AA^T = \begin{bmatrix} a_1 & b_1^T \\ b_1 & a_2 & b_2^T \\ & b_2 & a_3 & b_3^T \\ & & b_3 & a_4 \end{bmatrix}, \quad L = \begin{bmatrix} c_1 \\ d_1 & c_2 \\ & d_2 & c_3 \\ & & d_3 & c_4 \end{bmatrix} \quad (14)$$

The factorization is detailed in Algorithm 2.

² <https://github.com/UW-AMO/KalmanJulia>.

Algorithm 2 Block bi-diagonal Cholesky factorization for a block tri-diagonal positive definite matrix

Require: Input block diagonals $\{a_i\}$ and lower off-diagonals $\{b_i\}$ of block tridiagonal matrix AA^T (14).

- 1: $s_0 = 0, b_0 = 0$
- 2: **loop** $k = 1, \dots, N$
- 3: $s_k = a_k - b_{k-1}s_{k-1}^{-1}b_{k-1}^T$
- 4: $c_k = \text{chol}(s_k)^T$
- 5: $d_k = b_k c_k^{-1}$
- return** Diagonal blocks $\{c_i\}$ and lower-diagonal blocks d_i of block L (14)

Algorithm 2 is derived as follows. Multiplying out LL^T we have

$$a_1 = c_1 c_1^T, \quad d_1 = b_1 c_1^{-T}$$

To compute c_1 we need the standard Cholesky factorization of a_1 . Then

$$c_2 c_2^T = a_2 - b_1 a_1^{-1} b_1^T, \quad d_2 = b_2 c_2^{-1}.$$

For convenience, we introduce the recursively defined auxiliary terms s_k , with $s_1 = a_1$, and

$$s_k = a_k - b_{k-1} s_{k-1}^{-1} b_{k-1}^T.$$

Then each c_k is the standard Cholesky factorization of s_k , and d_k is immediately computed as in Algorithm 2. The overall complexity required for the single factorization is $O(n^3 N)$. Once L has been pre-computed, we need only $O(n^2 N)$ arithmetic operations to solve $LL^T \nu = Ac - \hat{w}$ for any right hand side. This is the same complexity as that of a matrix-vector multiply with A .

Local Linear Rate. When ρ is piecewise linear-quadratic [20,5], the DRS algorithm converges locally linearly to a solution, see Figure 2. More precisely, there is a real number $R > 0$ such that if $\|\eta^K - \eta^*\| < R$ then there is a constant κ with $0 < \kappa < 1$ such that for all $k > K$,

$$\|\eta^{k+1} - \eta^*\| < \kappa \|\eta^k - \eta^*\|,$$

where $\eta = \begin{bmatrix} z \\ \zeta \end{bmatrix}$, is the primal and dual pair.

Theorem 4.1 *Algorithm 1 converges with a locally linear rate.*

Proof: Following the proof technique of [14, Theorem 5], Algorithm 1 has a local linear convergence rate if the following two conditions are satisfied:

- (1) Algorithm (1) can be written as the action of a nonlinear operator satisfying a regularity property (see Lemma 4.2).

- (2) The functions g, ρ are *subdifferentially metrically subregular*³.

We show that these conditions hold for Algorithm 1. Define

$$Dx \mapsto \begin{bmatrix} \partial g(z) \\ \partial \rho^*(\zeta) \end{bmatrix}, \quad M = \begin{bmatrix} 0 & I \\ -I & 0 \end{bmatrix}, \quad H = \begin{bmatrix} \frac{1}{\tau} I & 0 \\ -2I & \frac{1}{\sigma} I \end{bmatrix}.$$

Define the nonlinear operator T by

$$T = (H + D)^{-1}(H - M). \quad (15)$$

T captures the iteration in Algorithm 1, which can be written as $\eta^k = T\eta^{k-1}$, for $\eta = \begin{bmatrix} z^T & \zeta^T \end{bmatrix}^T$. Then we have the following lemma.

Lemma 4.2 *Suppose that $\tau, \sigma < 1$. Then*

$$\|T\eta - \eta\|_{H-M}^2 \leq \langle \eta^* - \eta, (H - M)(T\eta - \eta) \rangle$$

where η^* is such that $0 \in (D + M)\eta^*$.

The proof is given in the Appendix.

This establishes condition (1). Condition (2) requires the concept of metric subregularity. This property is shown to hold for PLQ functions by [14] and [[6], Theorem 3.3]⁴ shows it is true for indicators of convex sets. This completes the proof of the theorem.

Comparison on Smooth Nonsingular Problems. If the covariances, Q, R are non-singular and the penalties $\rho_{1,2}$ are \mathcal{C}^1 -smooth, then the Kalman smoothing problem can be written as a smooth convex problem. In this case the same reformulation will work and algorithm 1 will still give a local linear rate. However more common algorithms such as gradient descent and L-BFGS can also be applied. We compare the performance of these three algorithms to track a particle moving along a smooth

³ A mapping $F : \mathbb{R}^n \rightrightarrows \mathbb{R}^m$ is called *metrically subregular* at \bar{x} for \bar{y} if $(\bar{x}, \bar{y}) \in \text{graph } F$ and there exists $\eta \in [0, \infty)$, neighborhoods \mathcal{U} of \bar{x} , and \mathcal{Y} of \bar{y} such that

$$d(x, F^{-1}\bar{y}) \leq \eta d(\bar{y}, Fx \cap \mathcal{Y}), \quad \forall x \in \mathcal{U}$$

⁴ **Theorem 3.3:** For a proper closed convex function f , the subdifferential ∂f is metrically subregular at \bar{x} for \bar{y} with $(\bar{x}, \bar{y}) \in \text{gra } \partial f$ if and only if there exists a positive constant c and a neighborhood \mathcal{U} of \bar{x} such that

$$f(x) \geq f(\bar{x}) + \langle \bar{y}, x - \bar{x} \rangle + cd^2(x, (\partial f)^{-1}(\bar{y})), \quad \forall x \in \mathcal{U}$$

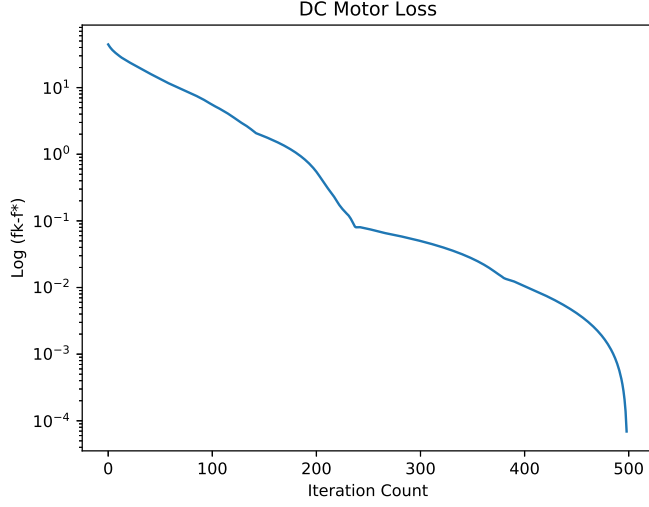


Fig. 2. Convergence rate for DRS splitting is locally linear when the objectives are piecewise linear-quadratic (PLQ). The convergence plot show here corresponds to the robust DC motor example in Figure 1.

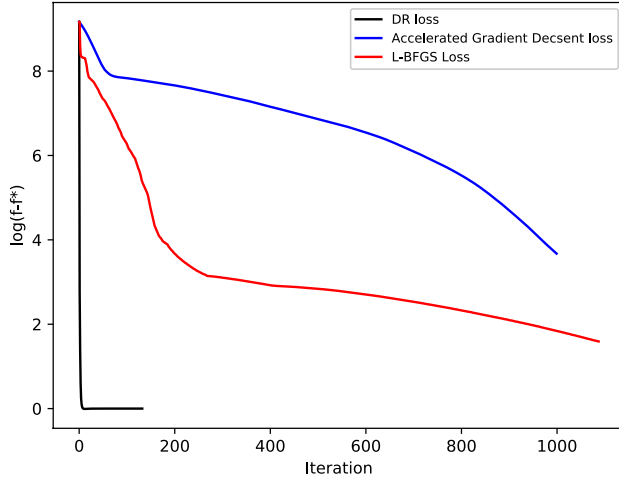


Fig. 3. Objective vs. iteration counts of Algorithm 1 for (12) (black), vs. accelerated gradient descent (AGD) (blue) and L-BFGS (red) for (3). Both ρ_1 and ρ_2 are Huber losses, with $\rho_3 \equiv 0$, and Q, R nonsingular, so (12) and (3) are equivalent. All iterations require $O(n^2N)$ operations. DRS splitting is much faster than methods with linear convergence rates and similar iteration complexity.

path. We use non-singular Q_k , and Huber penalty functions.

As seen in Figure 3, Algorithm 1 for (12) converges far faster than either accelerated gradient descent or LBFGS method on the equivalent nonsingular smoothing formulation (3). This is because its convergence rate does not depend on the condition number of the matrix A , so each iteration makes a lot of progress, and we can keep the complexity of each iteration at $O(n^2N)$, same as for a matrix-vector multiply needed for a gradient

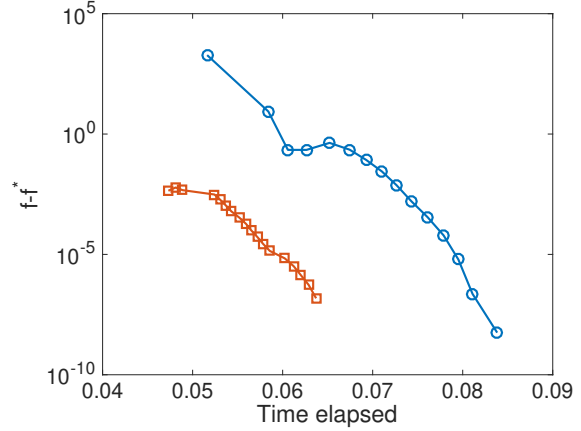


Fig. 4. Timed run of Algorithm 1 vs. IPsolve for the same setup as presented in Figure 3. At this scale, we see the locally linear convergence rate of the DRS. Even though IPsolve has superlinear rate, DRS wins because the slope of the rate is very steep, and each iteration is fast. By the time DRS is done, IPsolve has had time for only taken a few iterations.

ent evaluation, if we factor the sparse block tridiagonal matrix AA^T once at the start of the algorithm.

We also compare with the second-order interior point method, implemented in the IPsolve package⁵. Use-cases and performance of IPsolve for nonsingular Kalman smoothing is discussed in [4]. The results are shown in Figure 4, where IPsolve and DRS for the equivalent reformulation are compared for the nonsingular Huber-Huber Kalman model. Even though DRS has at best a linear rate, the constants are very good, as

⁵ <https://github.com/UW-AMO/IPsolve>.

they do not depend on the conditioning of the Kalman smoothing problem. The other advantage is that DRS can use a pre-factorized matrix, while IPsolve has to solve a modified linear system every time; there is no simple strategy to pre-factor as with DRS.

The numerical experiments suggest that Algorithm 1 should be used regardless of whether Q and R are singular or not. In the next section, we focus on a rich class of singular noise models found in navigation.

5 Navigation Models

Autonomous navigation requires high-fidelity tracking using occasional GPS and frequent depth/height, gyro-compass, and linear acceleration data. Gyro, compass, and linear acceleration are readily available from inertial measurement units (IMUs).

In this section, we develop a simple kinematic model that is trivially applicable to any vehicle, and is particularly appropriate for many underwater vehicle applications, where accelerations are heavily damped and autonomous vehicles often travel in long straight lines (e.g. for survey work). When the attitude is known or changing slowly, the model can be linearized effectively and the situation simplifies considerably. We give a brief description of the full nonlinear process model for a vehicle in Section 5.1, and derive the linear simplification in Section 5.2. Both our synthetic examples and underwater survey application use the linearized model.

5.1 Full Nonlinear Process Model

The complete state vector, denoted x , contains pose and attitude, as well as body-frame linear and angular velocities

$$x = [s^\top, \varphi^\top, v^\top, \omega^\top]^\top, \quad (16)$$

$$s = \begin{bmatrix} x \\ y \\ z \end{bmatrix}, \quad \varphi = \begin{bmatrix} r \\ p \\ h \end{bmatrix}, \quad v = \begin{bmatrix} u \\ v \\ w \end{bmatrix}, \quad \omega = \begin{bmatrix} a \\ b \\ c \end{bmatrix}, \quad (17)$$

where s is the vehicle pose in the local frame, φ is the vehicle attitude (Euler roll, pitch, heading), v is the body-frame linear velocity, and ω is the body-frame angular velocity. The simple kinematic process model for the vehicle is given by

$$\dot{x} = \underbrace{\begin{bmatrix} 0 & 0 & R(\varphi) & 0 \\ 0 & 0 & 0 & \mathcal{J}(\varphi) \\ 0 & 0 & 0 & 0 \\ 0 & 0 & 0 & 0 \end{bmatrix}}_{f(x(t))} x + \underbrace{\begin{bmatrix} 0 & 0 \\ 0 & 0 \\ I & 0 \\ 0 & I \end{bmatrix}}_G w \quad (18)$$

where $R(\varphi)$ is the transformation from body-frame to local-level linear velocities, $\mathcal{J}(\varphi)$ is the transformation from body-frame angular velocities to Euler rates, and $w \sim \mathcal{N}(0, Q)$ is zero-mean Gaussian process noise in the velocity term. $R(\varphi)$ and $\mathcal{J}(\varphi)$ are found by forming

$$R(\varphi) = R_h^\top R_p^\top R_r^\top \quad (19)$$

where R_h , R_p , and R_r are given by

$$\underbrace{\begin{bmatrix} ch & sh & 0 \\ -sh & ch & 0 \\ 0 & 0 & 1 \end{bmatrix}}_{R_h}, \underbrace{\begin{bmatrix} cp & 0 & -sp \\ 0 & 1 & 0 \\ sp & 0 & cp \end{bmatrix}}_{R_p}, \underbrace{\begin{bmatrix} 1 & 0 & 0 \\ 0 & cr & sr \\ 0 & -sr & cr \end{bmatrix}}_{R_r} \quad (20)$$

with $c\cdot$ and $s\cdot$ shorthand for $\cos(\cdot)$ and $\sin(\cdot)$; and

$$\omega = \begin{bmatrix} \dot{r} \\ 0 \\ 0 \end{bmatrix} + R_r \begin{bmatrix} 0 \\ \dot{p} \\ 0 \end{bmatrix} + R_r R_p \begin{bmatrix} 0 \\ 0 \\ \dot{h} \end{bmatrix} = \underbrace{\begin{bmatrix} 1 & 0 & -sp \\ 0 & cr & srsp \\ 0 & -sr & srsp \end{bmatrix}}_{\mathcal{J}^{-1}} \dot{\varphi}$$

where

$$\mathcal{J} = \begin{bmatrix} 1 & \sin r \tan p & \cos r \tan p \\ 0 & \cos r & -\sin r \\ 0 & \sin r \sec p & \cos r \sec p \end{bmatrix}. \quad (21)$$

5.2 Linear Process Model

For a vehicle that is well-instrumented in attitude, the uncertainty in position (and the x-y states in particular) is typically orders of magnitude larger than the uncertainty in attitude. In practice, we simplify the full nonlinear vehicle process model to track only position states (x, y, z) , while assuming that the attitude states (r, p, h) are directly available from the most recent sensor measurements. To make the model linear, the position and its derivatives are referenced to the local-level frame.

To incorporate linear acceleration measurements from an inertial measurement unit (IMU), we must track both linear velocities and linear acceleration in the state vector. This leads to the augmented state

$$x_s = [x, y, z, \dot{x}, \dot{y}, \dot{z}, \ddot{x}, \ddot{y}, \ddot{z}]^\top. \quad (22)$$

We still use a linear kinematic process model, which

now simplifies to

$$\dot{x}_s = \underbrace{\begin{bmatrix} 0 & I & 0 \\ 0 & 0 & I \\ 0 & 0 & 0 \end{bmatrix}}_{F_s} x_s + \underbrace{\begin{bmatrix} 0 \\ I \\ 0 \end{bmatrix}}_{G_s} w_s, \quad (23)$$

where $w_s \sim \mathcal{N}(0, Q_s)$ is zero-mean Gaussian process noise.

The linear process model (23) is discretized using a first-order Taylor series:

$$x_{s_{k+1}} = F_{s_k} x_{s_k} + w_{s_k} \quad (24)$$

$$F_{s_k} = e^{F_s T} \quad (25)$$

$$\begin{aligned} &= I + F_s T + \frac{1}{2!} F_s^2 T^2 + \frac{1}{3!} F_s^3 T^3 + \dots \\ &= \begin{bmatrix} I & IT & 0 \\ 0 & I & IT \\ 0 & 0 & I \end{bmatrix} \end{aligned}$$

where the higher order terms are *identically zero* because of the structure of F_s , resulting in a simple closed-form solution for F_{s_k} . The discretized process noise

$$w_{s_k} = \int_0^T e^{F_s(T-\tau)} G_s w_s(\tau) d\tau, \quad (26)$$

is a zero-mean Gaussian, with covariance given by

$$Q_{s_k} = \int_0^T e^{F(T-\tau)} G Q G^\top e^{F^\top(T-\tau)} d\tau, \quad (27)$$

which simplifies to

$$Q_{s_k} = \begin{bmatrix} \frac{1}{3} T^3 & \frac{1}{2} T^2 & 0 \\ \frac{1}{2} T^2 & T & 0 \\ 0 & 0 & 0 \end{bmatrix} Q_s, \quad (28)$$

for

$$e^{F(T-\tau)} = \begin{bmatrix} I & I(T-\tau) & 0 \\ 0 & I & I(T-\tau) \\ 0 & 0 & I \end{bmatrix}, \quad G = \begin{bmatrix} 0 \\ I \\ 0 \end{bmatrix}. \quad (29)$$

In this case Q_{s_k} has rank 2, because acceleration is modeled as an exact derivative of the velocity term. An al-

ternative is to use a rank 1 covariance model

$$Q^{1/2} = \begin{bmatrix} 0 & 0 & 0 \\ 1 & 0 & 0 \\ 0 & 0 & 0 \end{bmatrix} Q_s^{1/2},$$

as in the introductory example. Here we model acceleration as an exact derivative of velocity, and position as an exact integral of velocity, with velocity subject to random perturbations.

5.3 Measurement Models for the IMU

The inertial measurement unit (IMU) does not measure position or velocity, just linear and angular accelerations. To use these measurements, we track linear acceleration as part of the state. However, the acceleration measured by the IMU is relative to the physical frame of the vehicle, while the acceleration of the state is relative to the navigation frame. A coordinate transformation between these frames is required for a comparison.

The coordinate transformation is a well known function of the heading, pitch, and roll of the vehicle. For the simplified linear model, we pre-process heading, pitch and roll and then treat them as known quantities. The coordinate transformation is given by $R(\varphi)$, where φ comprises heading, pitch, and roll as described in Section 5.1.

Any navigation system that relies on the IMU needs occasional measurements that inform the position (e.g. GPS), otherwise the error in position estimates grows without bound. We assume that we are given such data from a separate source, sampled at a much lower update rate than the IMU. For any s where such data is available, we have the measurement model

$$H_s = \begin{bmatrix} I_{3 \times 3} & 0_{3 \times 6} \\ 0_{3 \times 6} & R(\varphi) \end{bmatrix}, \quad z_s = \begin{bmatrix} b^\top & \ddot{x}_{\text{meas}} & \ddot{y}_{\text{meas}} & \ddot{z}_{\text{meas}} \end{bmatrix}^\top.$$

If there is no position data measured at time s then we use the model

$$H_s = \begin{bmatrix} 0_{3 \times 3} & 0_{3 \times 6} \\ 0_{3 \times 6} & R(\varphi) \end{bmatrix}, \quad z_s = \begin{bmatrix} 0 & \ddot{x}_{\text{meas}} & \ddot{y}_{\text{meas}} & \ddot{z}_{\text{meas}} \end{bmatrix}^\top.$$

6 Analysis of Sea-Survey Data

Real data section will be added pending approval.

References

- [1] B. D. Anderson and J. B. Moore. *Optimal control: linear quadratic methods*. Courier Corporation, 2007. 1
- [2] B. D. O. Anderson and J. B. Moore. *Optimal Filtering*. Prentice Hall, 1979. 1, 2, 3
- [3] C. F. Ansley and R. Kohn. A geometric derivation of the fixed interval smoothing algorithm. *Biometrika*, 69:486–487, 1982. 2
- [4] A. Aravkin, J. V. Burke, L. Ljung, A. Lozano, and G. Pillonetto. Generalized kalman smoothing: Modeling and algorithms. *Automatica*, 86:63–86, 2017. 2, 3, 7
- [5] A. Y. Aravkin, J. V. Burke, and G. Pillonetto. Sparse/robust estimation and kalman smoothing with nonsmooth log-concave densities: Modeling, computation, and theory. *Journal of Machine Learning Research*, 14:2689–2728, 2013. 6
- [6] F. Artacho and M. Geoffroy. Characterization of metric regularity of subdifferentials. *Journal of Convex Analysis*, 15(2):365–380, 2008. 6
- [7] Y. Bar-Shalom, X. R. Li, and T. Kirubarajan. *Estimation with Applications to Tracking and Navigation*. John Wiley and Sons, 2001. 3
- [8] Y. Bar-Shalom, X. Rong Li, and T. Kirubarajan. *Estimation with applications to tracking and navigation*. John Wiley & Sons, Inc., New York, 2001. 1
- [9] B. M. Bell, J. V. Burke, and G. Pillonetto. An inequality constrained nonlinear Kalman-Bucy smoother by interior point likelihood maximization. *Automatica*, 45(1):25–33, Jan. 2008. 3
- [10] P. L. Combettes and J.-C. Pesquet. Proximal splitting methods in signal processing. In *Fixed-point algorithms for inverse problems in science and engineering*, pages 185–212. Springer, 2011. 5
- [11] R. J. Hyndman, A. B. Koehler, R. D. Snyder, and S. Grose. A state space framework for automatic forecasting using exponential smoothing methods. *International Journal of Forecasting*, 18(3):439–454, 2002. 1
- [12] A. Jazwinski. *Stochastic Processes and Filtering Theory*. Dover Publications, Inc, 1970. 3
- [13] R. E. Kalman. A New Approach to Linear Filtering and Prediction Problems. *Transactions of the AMSE - Journal of Basic Engineering*, 82(D):35–45, 1960. 2
- [14] P. Latafat, N. Freris, and P. Patrinos. A new randomized block-coordinate primal-dual proximal algorithm for distributed optimization. *arXiv preprint arXiv:1706.02882*, 2017. 6
- [15] L. Ljung. *System Identification - Theory for the User*. Prentice-Hall, Upper Saddle River, N.J., 2nd edition, 1999. 2
- [16] H. Ohlsson, F. Gustafsson, L. Ljung, and S. Boyd. Smoothed state estimates under abrupt changes using sum-of-norms regularization. *Automatica*, 48:595–605, 2012. 3, 4
- [17] B. Oksendal. *Stochastic Differential Equations*. Springer, sixth edition, 2005. 3
- [18] C. Paige. Computer solution and perturbation analysis of generalized linear least squares problems. *Mathematics of Computation*, 33:171–183, jan 1979. 2, 3
- [19] H. E. Rauch, F. Tung, and C. T. Striebel. Maximum Likelihood estimates of linear dynamic systems. *AIAA J.*, 3(8):1145–1150, 1965. 2
- [20] R. T. Rockafellar and R. J. B. Wets. *Variational Analysis*, volume 317. Springer, 1998. 6

- [21] R. S. Tsay. *Analysis of financial time series*, volume 543. John Wiley & Sons, 2005. 1

Appendix

6.1 Proof of Lemma 4.2.

Proof: As D is monotone we have

$$\langle \eta^* - T\eta, D\eta^* - DT\eta \rangle \geq 0$$

as $0 \in (D + M)\eta^*$ this implies

$$\langle \eta^* - T\eta, -M\eta^* - DT\eta \rangle \geq 0$$

Now $DT\eta = DT\eta + HT\eta - HT\eta = (H - M)\eta - HT\eta$.
Thus

$$\begin{aligned} 0 &\leq \langle \eta^* - T\eta, -M\eta^* + HT\eta - (H - M)\eta \rangle \\ &= \langle \eta^* - T\eta, -M(\eta^* - \eta) + H(T\eta - \eta) \rangle \\ &= \langle \eta^* - \eta, -M(\eta^* - \eta) + H(T\eta - \eta) \rangle \\ &\quad + \langle \eta - T\eta, -M(\eta^* - \eta) + H(T\eta - \eta) \rangle \end{aligned}$$

By definition of M we have

$$\langle M\eta, \eta \rangle = 0$$

for any η . Therefore

$$\begin{aligned} 0 &\leq \langle \eta^* - \eta, H(T\eta - \eta) \rangle + \langle \eta - T\eta, -M(\eta^* - \eta) \rangle \\ &\quad + \langle \eta - T\eta, H(T\eta - \eta) \rangle - \langle \eta - T\eta, M(T\eta - \eta) \rangle \\ &= \langle \eta^* - \eta, H(T\eta - \eta) \rangle + \langle \eta - T\eta, -M(\eta^* - \eta) \rangle - \|T\eta - \eta\|_{H-M}^2 \\ &= \langle \eta^* - \eta, H(T\eta - \eta) \rangle + \langle M(\eta - T\eta), \eta^* - \eta \rangle - \|T\eta - \eta\|_{H-M}^2 \\ &= \langle \eta^* - \eta, (H - M)(T\eta - \eta) \rangle - \|T\eta - \eta\|_{H-M}^2 \end{aligned}$$

6.2 Computing with Prox Operators

In this section, we collect the proximal operators used in the paper. From simple calculus, we have

- $\text{prox}_{\frac{\gamma}{2}\|\cdot\|^2}(z) = \frac{1}{1+\gamma}z$.

This generalizes to easily invertible least squares terms:

- $\text{prox}_{\alpha\frac{1}{2}\|Ax-b\|^2}(z) = (I + \alpha A^T A)^{-1}(\alpha A^T b + z)$.

For $\rho(z) = \delta_C(z)$, we have

$$\text{prox}_{\gamma\rho}(z) = \text{proj}_C(z).$$

This gives simple formulas for the following operators:

- $\text{proj}_{\gamma\mathbb{B}_2}(z) = \min(\|z\|, \gamma) \frac{z}{\|z\|}$.
- $\text{proj}_{\gamma\mathbb{B}_\infty}(z) = \min(\max(z, -\gamma), \gamma)$.
- $\text{proj}_{\mathbb{R}_+}(z) = \max(z, 0)$.

We also have fast implementations for the following operators:

- $\text{proj}_{\gamma\mathbb{B}_1}(z)$, the 1-norm projection
- $\text{proj}_{\gamma\Delta}(z)$, the scaled simplex projection
- $\text{proj}_{\gamma\Delta_1}(z)$, the capped simplex projection.

Next, the Moreau identity relates the prox operators for f and f^* :

$$\text{prox}_{\alpha f^*}(z) = z - \alpha \text{prox}_{\alpha^{-1}}(\alpha^{-1}z)$$

This identity together with previous results yields the following operators:

- $\text{prox}_{\gamma\|\cdot\|_2}(z)$
- $\text{prox}_{\gamma\|\cdot\|_1}(z)$
- $\text{prox}_{\rho_n}(z)$, prox of hinge loss.
- $\text{prox}_{\gamma\|\cdot\|_\infty}$

Often we add a simple quadratic to a penalty; the prox of the sum can be expressed in terms of the prox of the original penalty.

- $\text{prox}_{\alpha(f + \gamma/2\|\cdot\|^2)}(x) = \text{prox}_{\frac{\alpha}{1+2\alpha\gamma}f}\left(\frac{1}{1+2\alpha\gamma}x\right)$.

This immediately gives the prox of the elastic net, which is the sum of the 1-norm and a simple quadratic.

Likewise, we can compute the prox of a Moreau envelope of a given penalty.

- $\text{prox}_{\gamma e_\alpha \rho}(z) = \frac{\alpha}{\gamma+\alpha}z + \frac{\gamma}{\gamma+\alpha}\text{prox}_{(\gamma+\alpha)\rho}(z)$

This immediately gives us formulas for prox of the Huber, as well as smoothed variants of any other penalty in the collection.